MODELING AND EXPERIMENTAL TESTING OF THE EFFECT OF SOLVENT ABSORPTION ON THE ELECTRIC PROPERTIES OF SBR/CB CHEMICAL SENSORS

Antonio Carrillo, Ignacio R. Martín-Domínguez, Rigoberto Ibarra and Alfredo Márquez*
Centro de Investigación en Materiales Avanzados, S. C. (CIMAV), Miguel de Cervantes 120, Complejo Industrial Chih., 31109, Chihuahua, Chih., México.

1. INTRODUCTION

A number of chemical sensors are designed employing polymeric matrices filled with carbon particles (Carbon black, graphite or even carbon nanotubes). These matrices may be single polymers [1-4,] or blends [5]. These sensors work on the basis of a change on their electric properties when they come in contact with a specific substance. Their electric properties are in general dictated by the electric percolation of the carbon particles into the composite. When the carbon/polymer composites come into contact with a substance that is chemically compatible with the polymeric matrix, its conductivity gradually decreases with the exposure to this substance. This process is associated to a change in the volume of the polymer matrix caused by the absorption and diffusion of the solvent, which causes a reduction of the carbon particles volumetric fraction relative to the non-conductive material (polymer matrix plus organic solvents). This reduction results in an increase of the distance between carbon clusters and the subsequent breaking of the percolative chains, with the associated decrease in the composite's conductivity.

In a previous work [6], the influence of swelling by solvent absorption on the electrical properties of elastomers filled with carbon particles was theoretically studied. It was found that diffusion dynamics have a very important effect on the evolution of the electrical conductivity of these composites once they come into contact with solvents. The previous model is tested in this work using Styrene-Butadiene Rubber (SBR) filled with carbon particles. The objective of the model is to relate the percolation theory with the solvent diffusion equation in amorphous polymers, in order to improve the performance of chemical sensors made with similar materials.

Finally, it is important to mention that the percolative relationship between the electrical resistivity and volumetric fraction of conductive aggregates in a polymer composite has been widely analyzed both theoretically and empirically (52-75). However, this relationship has always been studied in homogeneous composites, where the distribution of the conductive fraction is uniform. There is, however, a wide range of phenomena in which the conductive fraction varies significantly within the polymer, especially when gaseous or liquid solvents are being absorbed by a polymer matrix. This phenomenon has an important application in designing chemical sensors and artificial odor detection systems.

* Corresponding author; e-mail address: alfredo.marquez@cimav.edu.mx

2. EXPERIMENTAL PROCEDURE

S1205 Poly-Styrene-Butadiene rubber (SBR), manufactured by *Negromex*, was chosen as the matrix to prepare the composite samples. SBR was loaded with a mixture of carbon black (CB) particles (Vulcan XC72, provided by *Cabot Inc.*) and type O Graphite, provided by *Grafito de México*. All samples were prepared with a CB/Graphite weight ratio of 1.0:1.4. Tests were performed in a special chamber represented in Fig.1. In these tests, the samples connection area was isolated from the solvents by means of hermetic polyethylene capsules manufactured especially for the test. These capsules prevented the entrance of solvent into the electrode area, thus eliminating eventual contact problems and interference during the measurements. The effective length of the samples that was exposed to the solvents was 30.0 cm. The previous arrangement was placed in a glass recipient, where a tension of 1.0 volt was applied to the samples using a constant voltage power source, a *BK PRECISION (DINASCAN),* model 1601. The current that circulated through the sample was continually registered by a *Cole Parmer* register (model 2030-0000). Once the previous circuit reached a steady state, 1.0 L of solvent was poured into the recipient, completely covering the samples. To evaluate the samples dimension increase due to the diffusion of the solvents, they were periodically photographed with a *Canon* camera (model EOS 1000 FN), whose lens was focused on the central part of the sample (Fig. 1). With the purpose of estimating the sample's length increase, two reference marks with a separation of 1.8 cm were drawn on them and photographed. Once the samples were in contact with the solvent, they were photographed every 3 min (Fig. 2). All the tests were performed at room temperature (25.0 ± 2°C), and the following solvents were selected for them: tetrahydrofurane (THF), benzene, xylene, diethyl ether, and hexane, all of which were provided by *Aldrich*. Unleaded gasoline, commercialized as *Magna-Sin* by *Petroleos Mexicanos* (PEMEX), was used as well.

3. RESULTS AND ANALYSIS

Fig. 2 illustrates how the samples swell when are immersed in a solvent. It is observed that the diameter increases in a 38% while the length only in 6.25%. This behavior is apparently due to the resistance of the almost dry center of the sample to elongate longitudinally during the swelling of external layers. Now, considering that elastomers in general follows the diffusion Fick's Law [8], it is possible to use the following expression to determine the solvent volumetric fraction $f_{S,}(r,t)$ diffused into the sample;

$$\frac{\partial f_S(r,t)}{\partial t} = \mathrm{D}\,\nabla^2 f_S(r,t) + \nabla D \cdot \nabla f_S(r,t) \qquad (1)$$

where D is the diffusion coefficient related to the volumetric fraction. This coefficient in the case of polymers may become concentration-dependent for large swelling levels. However, the treatment of D is possible in closed form only if the variation of D with f_S is known *a priori* and it is possible to express this variation analytically [76]. Therefore, as

a first approach D is considered a constant in the present study. Taking into account this hypothesis the last expression may be written as:

$$\frac{\partial f_S(r,t)}{\partial t} = \frac{D}{r}\frac{\partial}{\partial r}\left(\mathrm{r}\frac{\partial f_S(r,t)}{\partial r}\right) \tag{2}$$

To solve this equation, the following initial and boundary conditions apply:

$$\begin{aligned} &f_S(r,0) = 0,\ 0 \le r < a(0) \\ &f_S(r,t) = f_{S\max},\ r = a(t),\quad t \ge 0 \end{aligned} \tag{3}$$

where f_{Smax} is the maximum solvent volumetric fraction that the composite is able to absorb. The general solution of Eq. 2, subject to conditions specified by Eqs. 3, is [8]:

$$f_S(r,t) = \left(1 - \frac{2}{a(t)}\sum_{n=1}^{\infty}\frac{\exp(-\mathrm{D}\alpha_n^2 t)\,J_0[r\alpha_n]}{\alpha_n J_1[a(t)\alpha_n]} + \ldots.\right) f_{S\max} \tag{4}$$

where J_0 and J_1 are the first class Bessel functions of zero and first order, respectively, and both α_n are the positive roots of $J_0[a(t)\,\alpha_n]$. Finally, the following relation was derived to evaluate the increment of the filament external radius:

$$a^2(t) = a^2(0) + 2\int_0^{a(t)} f_S(r,t)\,r\,dr \tag{6}$$

It is apparently impossible to obtain an explicit expression for $a(t)$ using Eqs. 4, 5 and 6; however, it is possible to evaluate this parameter using a numerical method. To numerically evaluate Eqs. 4 through 6, the sample radius was divided into a number of segments, n > 20 (bi-dimensional rings), as illustrated in Fig. 3. Using this partition, Eq. 6 can be expressed as:

$$0 = a^2(0) - a^2(t) + \sum_{i=1}^{n} f_S(r_i^2 - r_{i-1}^2); \tag{7}$$

where

$$r_n = a(t) \ \ and \ \ r_0 = 0$$

In this equation, $a(t)$ is calculated by using a Newton-Raphson method, where Eq. 7 is linked to Eq. 4 for large times and to Eq. 5 for short ones. More specifically, for long time periods Eqs. 4 and 7 were fitted to the experimental data in order to assess the D and $f_{s,max}$ values, while equations 5 and 7 were used for short time periods. The curve fitting process was based on minimizing the sum of the absolute differences between experimental and calculated values, using a multivariable Newton-Raphson algorithm. Since the external filament radius is growing with time, because of solvent-sample contact, the problem becomes one with moving boundary conditions.

Fig. 4 shows the experimental swelling data from six different solvents, as well as the fitting of Eq. 7 to this data using the diffusion coefficients D and $f_{s\ max}$ reported in Table 4. It must be noted that the composite's behavior is very well described by our model.

Now in order to model the samples electric behavior, the following hypotheses were assumed:

i) The elastomer matrix and the organic solvents are dielectric materials.
ii) Solvents are absorbed only by the polymeric matrix and not by the conductive aggregates.

Using these hypotheses, it is possible to predict the variation of the electric current in the composite during the solvent diffusion process (provided that the voltage is constant). First of all, by taking in account the cylindrical geometry of the samples Ohm's law can be written as:

$$I(t) = \int_{o}^{a(t)} \frac{2\pi \cdot r \cdot V}{\rho_m(r,t) \cdot l(t)} dr \qquad (8)$$

where r *is* the radial coordinate, $I(t)$ and $\rho_m(t)$ are the instantaneous electric current and local resistivity, and $a(t)$ and $l(t)$ are their external radius and sample length, respectively. Finally, V is the applied voltage, which remains constant.

Equation 8 can be normalized as:

$$\frac{I(t)}{I_0} = \frac{2l_0}{r_0^2} \int_{0}^{a(t)} \frac{\rho_{m0}}{\rho_m(r,t)} \cdot \frac{r(t)}{l(t)} dr \qquad (9)$$

where the variables indexed with zero represent the state of the composite before that the solvent comes into contact with it. As previously mentioned the sample length increases very few during the test (~6%), see Fig. 2, because the almost dry center of the sample works as a reinforcement. Therefore, it is evident from Eq. 9 that the current intensity falls because the composite resistivity $\rho_m(r,t)$ increases with time during the test. In order to calculate the composite resistivity, it is necessary to know its relationship with the solvent volumetric fraction. This can be calculated by modifying a model proposed by McLachlang et al [7], which describes the conductive composite's electric resistance change as a function of its conductive and dielectric volumetric fractions. This equation, which is known as the generalized effective media (GEM) model, integrates two morphology parameters: f_C (the critical percolative value of the conductive fraction) and q (an experimental exponent). The previous equation can be written as:

$$\frac{(1-f)\left(\rho_H^{-1/q} - \rho_m^{-1/q}\right)}{\rho_H^{-1/q} + f_R \rho_m^{-1/q}} + \frac{f\left(\rho_L^{-1/q} - \rho_m^{-1/q}\right)}{\rho_L^{-1/q} + f_R \rho_m^{-1/q}} = 0 \qquad (10)$$

where ρ_H and ρ_L are the resistivities of the high and low resistive components, respectively, ρ_m is the composite resistivity, f is the conductive fraction and f_R is given by the following expression:

$$f_R = \frac{1-f_C}{f_C} \qquad (11)$$

Solving Eq. 10 for ρ_m, we have (see Annex A):

$$\rho_m = \{½\,[B \pm (B^2 + 4C)^{1/2}]\}^{-q} \qquad (12)$$

where

$$B = f_R^{-1}\,[(f f_R + f - 1)\rho_L^{-1/q} - (f f_R + f - f_R)\rho_H^{-1/q}],$$

$$C = f_R^{-1}\,(\rho_L\ \rho_H)^{-1/q} \qquad (13)$$

The positive sign of Eq. 12 is used to describe the behavior of a composite in which the conductive fraction is larger than the critical percolative fraction (f_C), while the negative sign is used for composites in which the smaller than f_C. Therefore, only the positive sign of the previous equation will be used in this work.

It is important to mention that the GEM equation was deduced for a composite of only two components. However, it can be used if the following assumption is accepted: since the polymer matrix and the organic solvents are both dielectric and have significantly larger resistivities than the conductive carbon fraction, both components (polymer and solvent) may be electrically treated as one same component. Therefore, the sum of the polymeric matrix fraction (f_P) plus the solvent fraction (f_S) will be named "the non conductive fraction (f_{nc})". This approximation is possible because the resistivity is a physical magnitude that presents one of the broadest ranges of values. While the resistivity of common organic substances varies between 10^{16} and 10^{8} ohms-cm, the conductive aggregates have conductivities between 10^{-1} and 10^{-7} ohms-cm. The conductive fraction is expressed by:

$$f(r,t) = 1 - f_{nc}(r,t) \qquad (14)$$

To evaluate $f(r,t)$ in each location as a function of time, the following relation was considered:

$$f(r,t) = 1 - f_P(r,0)\cdot[1 - f_S(r,t)] - f_S(r,t) \qquad (15)$$

Using the previous equations, it is possible to calculate $f(r, t)$ using the value of $f_S(r, t)$ from Eqs. 4 or 5.

Now, before to evaluate the influence of solvents we need to evaluate the percolation curve of the composite. This has been performed employing the second set of samples (which composition is reported in Table 4). Fig. 5 illustrates how the resistivity of these last samples dramatically diminishes when the fraction of conductive particles increases. In the same figure, the best fitting to the GEM equation (Eq. 12) is represented by a continuous line. It is observed that the GEM model fits reasonably well to experimental data. The q and f_C parameters of these composite were calculated as: 4.5 and 0.1434, respectively.

Returning to the first set of samples, their electric resistivity at each location (ρ_i) is then calculated from Eqs. 12 and 15, and the evolution of the current intensity throughout the sample can be evaluated with the following equation:

$$\frac{I(t)}{I_0} = \frac{l_0}{l(t)\cdot a(t)_0^2}\sum_{i=1}^{n}\left(\frac{\rho_0}{\rho_i(t)}\right)\left(r_i^2 - r_{i-1}^2\right)$$

where (15)

$$r_n = a(t)\ \ and\ \ r_0 = 0$$

The estimated ratio $I(t)/I_0$ may be now compared with the experimental values.

Fig. 6 illustrates how the electric current falls with the solvent contact time for each different solvent. The predictions of the model are represented with a continuous line in this graphic. Fig. 6.a groups the cases where the predictions of the model are closest to the experimental data, while Fig. 6.b assembles the rest. It can be noted that the less polar solvents (Hexane and Benzene) and Diethyl ether are poorly described by the model. It is important to note that these solvents are also those which produce the faster dropping rates of current intensity.

Finally, it must be mentioned that trying to get a better fit to the experimental results, we employed different approaches to describe the percolation curve (78-80), besides the model of McLachlan, however the results were so similar that we neglected the differences between them.

5.- DISCUSSION.

First of all, it is important to observe that our model describes very well the swelling of the samples (Fig. 4), showing that this composite obeys closely the Fick's diffusion model. As previously mentioned this agreement could fail at large swelling levels where the diffusion coefficient becomes concentration dependent, however during our tests it was not the case. Moreover, it was observed that the electrical behavior of the samples due to swelling is only qualitatively described (Fig. 6), and that the model slightly underestimates the drop rate of current intensities.

Now, as the morphology, structure and preparation method of the samples are the same, as well as the test temperature and pressure, and the electrical properties of the solvents are similar, it is very intriguing why this model that describes so well the swelling data and percolation curve of the composites, finishes for underestimates the swelling effect in almost all the cases. Indeed, at the exception of the case of THF, the dropping rates of the current intensity were underestimated (at this respect it is important to remark that the THF is also the solvent that fastest swells the samples.)

A possible explanation to this result is that the diffusion of solvents may be faster at the carbon/SBR interface than at the bulk of the SBR. Thus the interface would works like a preferential area for the flow of these solvents. Indeed, as has been signaled by Vesely [9] and Montes [10] voids are formed at this type of interfaces which can facilitate the local flow of the solvents. Then, the swelling rate around the percolative chains could be faster than the average rate of the composite. This effect may produce the early opening of these chains and the faster dropping rates experimentally observed. So, in the case of THF the diffusion rate at the interface may be of the same order of magnitude than at the SBR bulk given as a result that the effect of this solvent is in good agreement with the model. Also, it is interesting to mention that; when the samples are removed from the solvent, they starts to desorb it and consequently their conductivities are re-established gradually. This happens for all the samples at the exception of these corresponding to diethyl ether which remains non conductive. A careful examination of these last samples showed a series of transversal fissures produced by the solvent. It is important to remember that is precisely the diethyl ether that produces the fastest drop of the current intensity (even thought it produces a

mediocre swelling.) So, it is possible that these fissures have been formed due to the excessive concentration of solvent at the carbon/SBR interface.

Moreover, it is true that SBR molecules at the interface could have a saturation swelling smaller than bulk molecules [82], because they can be anchored in a certain degree to the carbon particles; however, they could swell faster due to the probable presence of solvent at the early stages of the test.

In order to elucidate the previous theory, currently we are carrying out a series of tests with elastomer blends employing different content of carbon particles. The influence of the interfaces must be larger in these tests providing more information about this interesting phenomenon. Also, we are developing a more sophisticated model in order to demonstrate the previous theory.

Finally, it is important to stress that; even though the present model only predicts qualitatively the electric behavior of the samples it has the merit to show the existence of second order phenomena unseen until now.

6. CONCLUSION

A model that describes the swelling and electric behavior of carbon/elastomer composites during solvent diffusion processes is introduced in this work. The equations that result from this method take care of the problem of moving boundaries characteristic for polymer swelling, requiring simple numerical procedures to be solved and no numerical instability was observed during the calculation. The experimental swelling behavior of the samples is very well described for the model; however it slightly underestimates the rate at which the sample's resistivity increases with the solvent swelling, given just a qualitative approximation of this last phenomenon. This deficiency could be due to a preferential diffusion of solvents in the carbon/SBR interface that produces a faster resistivity increase than this predicted by the model. Finally, it is important to mention that this model provides a qualitatively proper description of the swelling and electric behavior of all the solvents, giving a good approximation of the performance of a polymer sensor. It is evident that this model is still incomplete and must be improved, but currently has the merit to describe the involved phenomena in the correct direction.

10. REFERENCES.

1.	Y.P. Mamunya, H. Zois, L. Apekis, E.V. Lebedev, Influence of pressure on the electrical conductivity of metal powders used as fillers in polymer composites, *Powder Technology*, 140 (2004) 49-55.
2.	M. Knite, V. Teteris, A. Kiploka, J. Kaupuzs, Polyisoprene-carbon black nanocomposites as tensile strain and pressure materials, *Sensors and Actuators, A: Physical,* A110 (2004) 142-149.
3.	M. Knite, V. Teteris, B. Polykov, D. Erts, Superconductive carbon-black polymer composite as prospective deformation sensor material. Investigations on macro and nanoscales. *Materialzinatne un Lietiska Kimija,* 2 (2001) 39-47.
4.	J. S. Park, P.H. Kang, Y.C. Nho, Characterization of carbon black filled polymer composites for strain sensor, *J. Ind. Eng. Chem.,* 9 (2003) 595-601

5.	J.F. Feller, Conductive polymer composites: influence of extrusion conditions on positive temperature coefficient effect of poly(butylenes terephthalate)/ poly(olefin) -carbon black blends, *J. Appl. Polym. Sci.,* 91 (2004) 2151-2157.
6.	A. Carrillo, I. Martin-Dominguez, A. Rosas, A. Marquez-Lucero, Numerical method to evaluate the influence of organic solvent absorption on the conductivity of polymeric composites, *Polymer,* 43 (2002) 6307-6313.
7.	M. Blaszkiewcz, D. McLachlang, R.E. Newnham, The volume fraction and temperature dependence of the resistivity in carbon-black and graphite polymer composites: An effective media percolation approach, *Polym. Eng. and Sci.,* 32 (1992) 421.
8.	J. Crank, The Mathematics of Diffusion, Uxbridge, UK: *Oxford Science Publications,* 1986, p. 73
9.	Vesely, D., Molecular sorption mechanism of solvent diffusion un polymers, *Polymer,* 42 (2002), 4417-4422.
10.	J. Berriot, F. Lequeux, H. Montes, H. Pernot, Reinforcement of model filed elastomers: experimental and theoretical approach of swelling properties, *Polymer*, **43** (2002) 6131-6138.

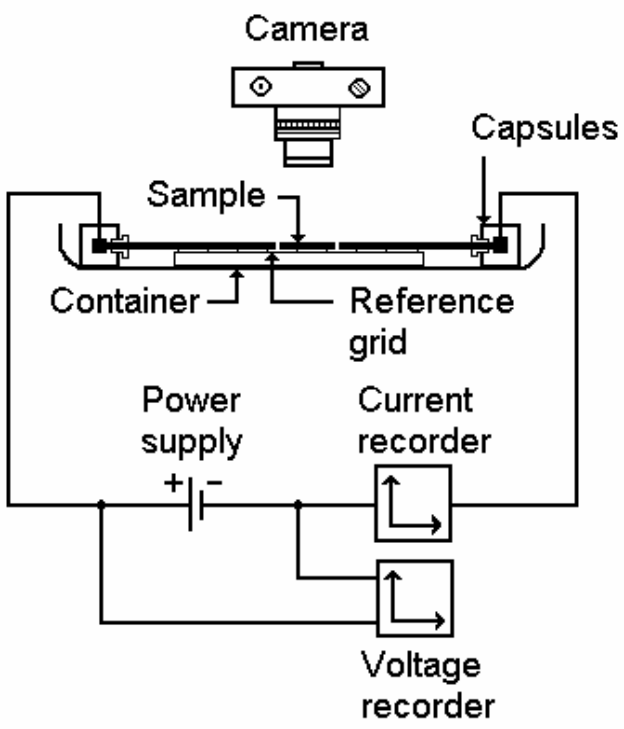

Figure 1. Sketch of the circuit for sensor testing.

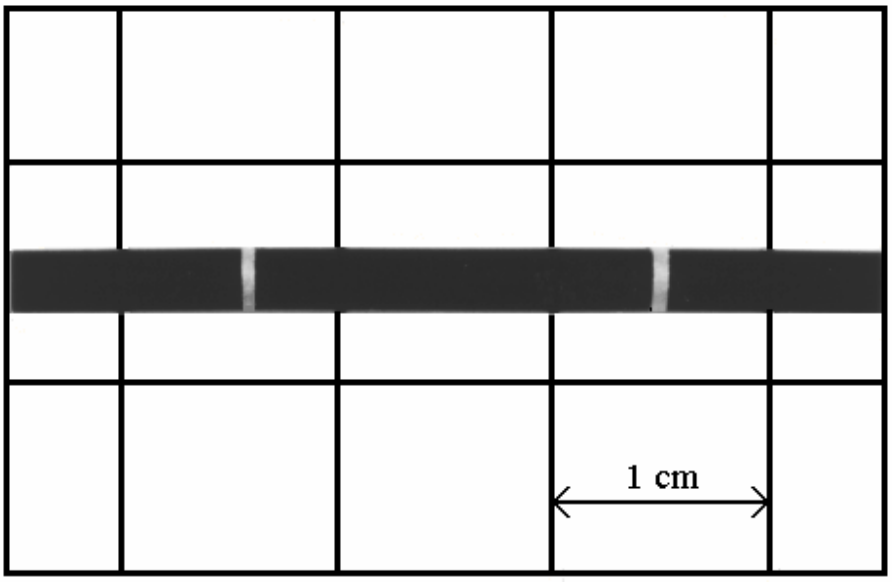

a)

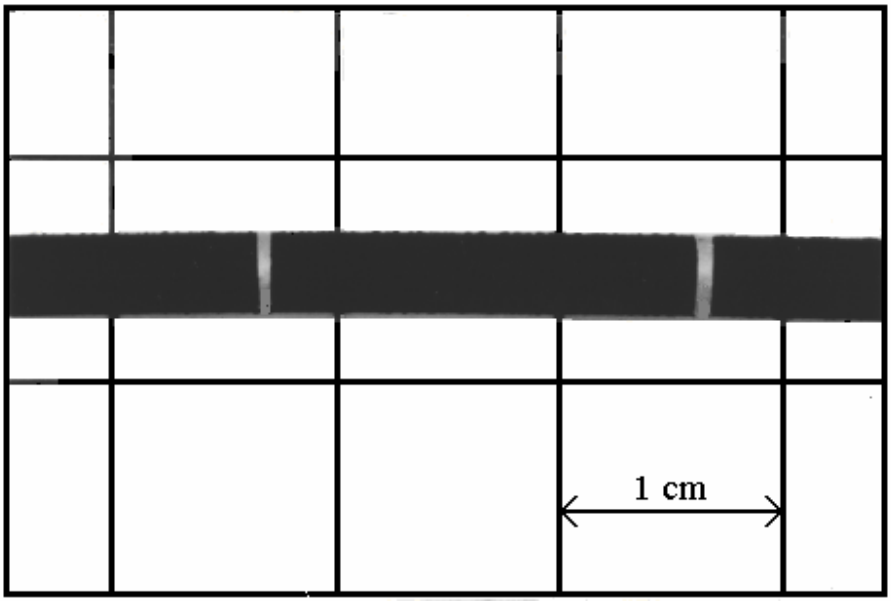

b)

Figure 2. Photographs of the samples swelling. a) Original sample. b) After 18 min of immersion in Benzene

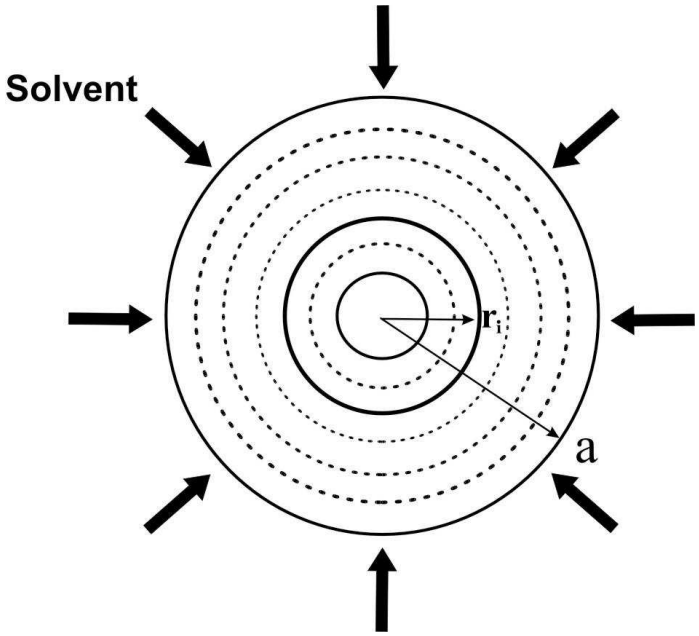

Figure 3. Partition of the sample section in a number of discrete layers.

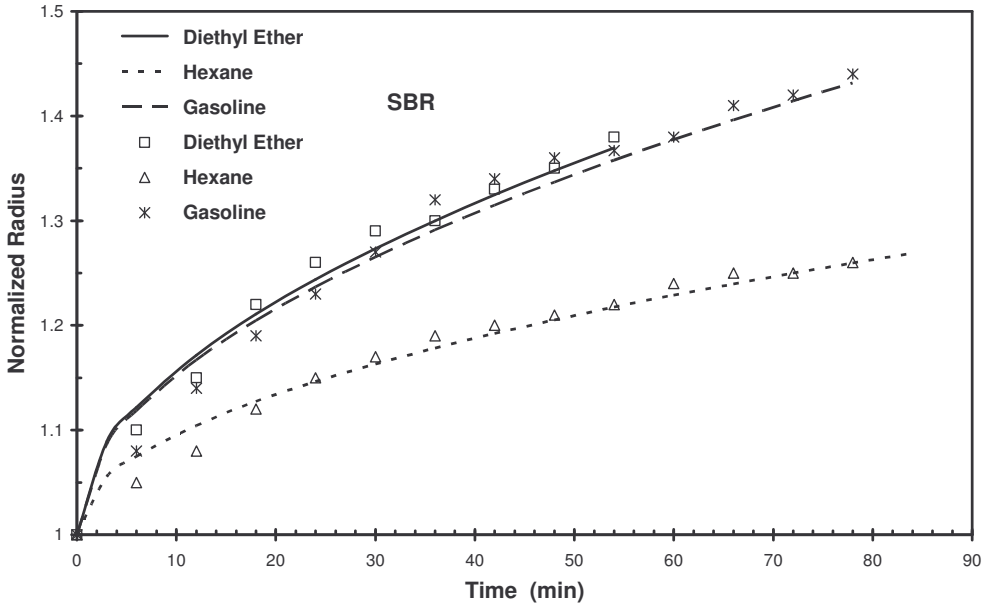

a)

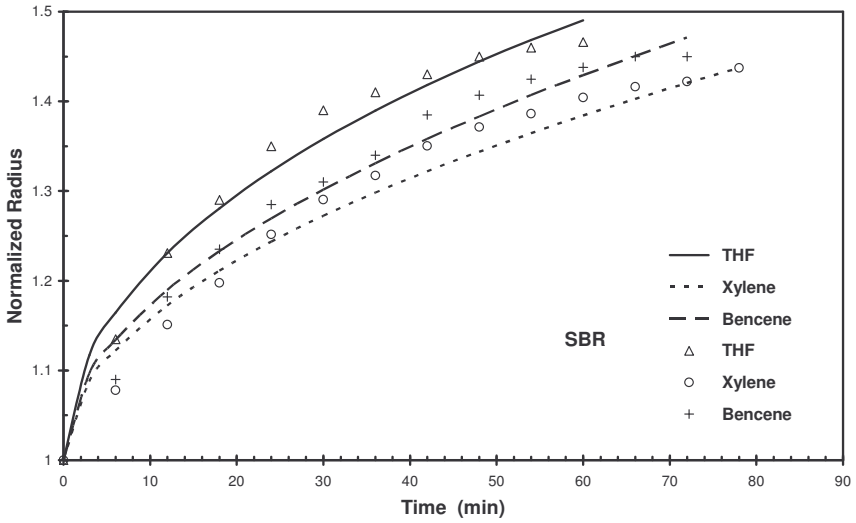

b)

Figure 4.- Evolution of the instantaneous radii for different solvents (the continuous line corresponds to the predictions of the present model).

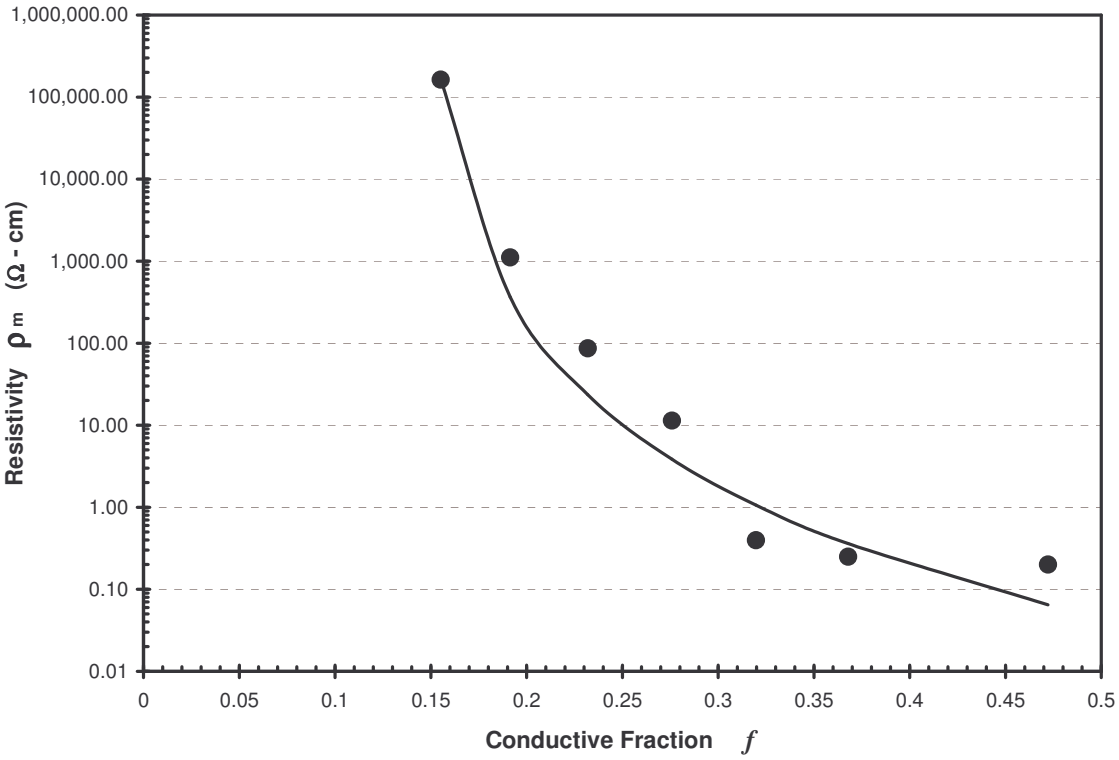

Figure 5.- Percolation curve for SBR/Carbon composites (the continuous line corresponds to the GEM model).

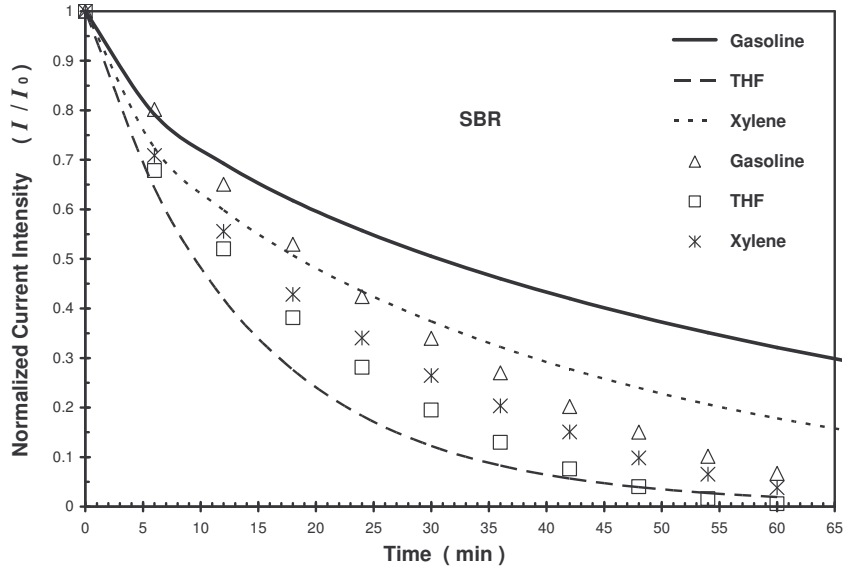

(a)

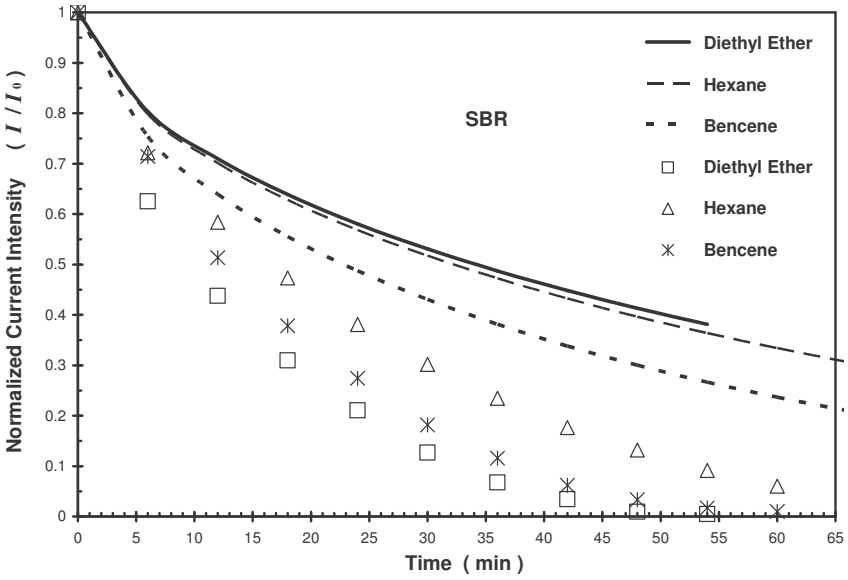

b)

Figure 6.- Falling of the current intensity with the solvent contact time (the continuous line corresponds to the present model).